Proceedings of the 10th Brazilian Congress of Thermal Sciences and Engineering -- ENCIT 2004
Braz. Soc. of Mechanical Sciences and Engineering -- ABCM, Rio de Janeiro, Brazil, Nov. 29 -- Dec. 03, 2004

Paper CIT04-0079

CHARACTERIZATION OF THE FLOW BEHIND A CONICAL SHOCK WAVE TO EVALUATE THE OPERATIONAL CONDITIONS OF A SUPERSONIC COMBUSTION RESEARCH FACILITY

Valéria Serrano Faillace Oliveira Leite
Instituto de Estudos Avançados (IEAv / CTA) - São José dos Campos, SP, CEP: 12228-840.
valeria@ieav.cta.br

Paulo Afonso de Oliveira Soviero
Instituto Tecnológico de Aeronáutica (ITA) - São José dos Campos, SP, CEP: 12228-900.
soviero@aer.ita.br

Abstract: In order to evaluate the operational conditions of a direct-connect supersonic combustion research facility, it was necessary to study the flow behind the shock waves over cones and wedges considering the effects of high velocities and high temperatures. The facility consists basically of a vitiated air unit and a nozzle directly coupled to the supersonic combustor to be tested. The flow at the combustor inlet should simulate the conditions of the air behind the oblique or conical shock waves over wedges, cones or other axially symmetric bodies used to compress the free stream flow in supersonic combustion air breathing systems like scramjets or ram accelerators. The nozzle is designed to generate the desired Mach number and the high air temperature is obtained in the vitiated air generator by combustion. The condition at the exit of the nozzle (the entrance of the combustor) should be the same as the flow behind the shock wave formed in front of the edge of wedges or the vertex of cones, flying in supersonic or hypersonic velocities. In this paper will be presented the analyses of the flow field over a cone at zero angle of attack, flying with hypersonic velocity, using three gas models: a calorically perfect, a thermally perfect and an equilibrium high-temperature one. The resulting system of ordinary differential equations is solved numerically by a Runge-Kutta method. Comparisons between the results provided by the three models will be discussed in order to evaluate the influences of high Mach numbers on the main flow variables.

Keywords: *Conical Flow, Hypersonic Flow, Supersonic Combustion Research Facility.*

1. Introduction

Supersonic combustion researches and hypersonic flow studies require ground test facilities such as shock tunnels, light gas guns (LGG) and supersonic combustion ramjet (scramjet) test benches (Dunsworth, 1979). Among these facilities the Institute for Advanced Studies (IEAv) of the Aerospace Technological Center (CTA), in São José dos Campos, has a hypersonic shock tunnel, which has been used, since 1992, for many experiments where the simulation of hypersonic flow conditions have been necessary. To complete the set of ground test facilities for the supersonic combustion studies the Combustion and Propulsion Laboratory (LCP) of the National Institute for Space Research (INPE), in Cachoeira Paulista, is assembling a scramjet combustor test bench with a vitiated air generator (VAG) coupled to a nozzle, for the testing of supersonic combustors and their components, as shown in the schematic drawing in Fig. (1).

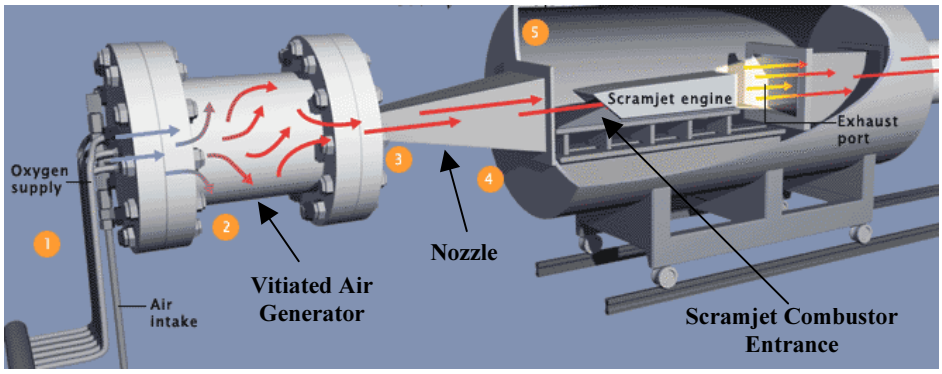

Figure 1: Schematic drawing of the supersonic combustion research bench.

The scramjet test facility, which is now being assembled in LCP/INPE, with the IEAv/CTA, is a continuous flow direct-connected type, providing combustor inlet flow conditions corresponding to flight Mach numbers ranging from 6 to 8. The flow at the combustor entrance must simulate the conditions of the air behind the oblique or conical shock waves formed at the nose wedge, one of the shapes of the body used to compress the free stream, or in front of the nose cone of ram accelerators, operating in the super detonative mode (Hertzberg, 1988).

As it is well known, the air (hypersonic flow) entering the intake of a scramjet is slowed to supersonic speeds, by compression of the air against an oblique or conical surface in the entrance of the combustor (Heiser, 1994). Fuel (H_2 or a hydrocarbon) is injected into the supersonic stream, where it mixes and burns in a combustion region downstream of the fuel injector strut. The expansion of hot gases through a supersonic nozzle at the back end of the engine, after fuel injection and combustion, accelerates the exhaust gas to a velocity higher than that of the inlet, generating thrust. The scheme of a scramjet combustor is shown in Fig. (2).

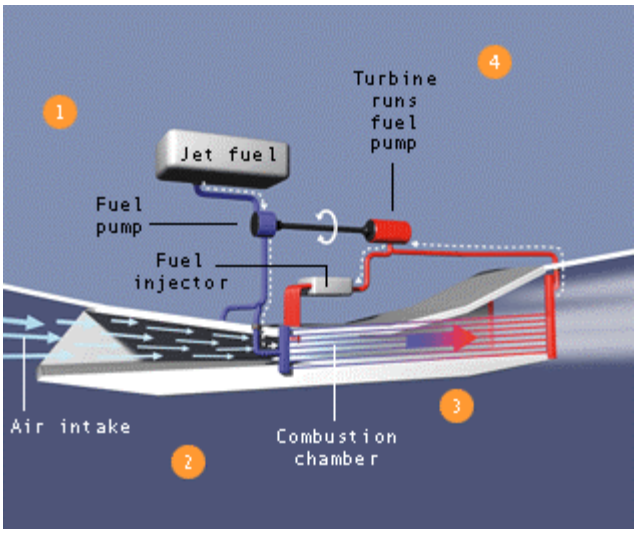

Figure 2: Scramjet combustor scheme.

To simulate the same conditions of the air in the entrance of a scramjet combustor, in a ground test facility shown in Fig. (1), oxygen enriched air should be heated, by combustion, inside the vitiated air generator and then accelerated through the nozzle, thus feeding the combustor, under testing, with a "vitiated air" containing the desired flow properties, plus the combustion products, generated in the heating process, while keeping the desired atmospheric oxygen content.

The heart of the direct-connected scramjet combustor test facility is the vitiated air generator (VAG). It consists of an axisymmetric cylindrical chamber where the air is first enriched with oxygen and then heated by the combustion of a fuel, yielding the desired stagnation temperature before passing through a nozzle to be accelerated to the desired Mach number. Figure (3) shows the complete scheme of a VAG. The fuel injection plate and the enriched air diffuser are assembled in one side of the combustion chamber. On the other side there is a nozzle, which will be directly connected to the scramjet combustor to be tested. Early work in this field was done in Brazil during the nineties, dealing with a preliminary vitiated air generator with 200.00 mm of diameter and 900.00 mm long (Guimarães et al, 1993; 1996; jul/1997 and dec/1997). This first equipment allowed the evaluation of the efficiency of the whole system and the validation of design concept of the injection plate for liquid fuel.

The results obtained with the first system led to the construction of a second one, which has a larger diameter (310.00 mm), is longer (1,500.00 mm) and is water cooled, as shown in Fig. (3), to assure the mechanical integrity of the material during longer and more frequent tests.

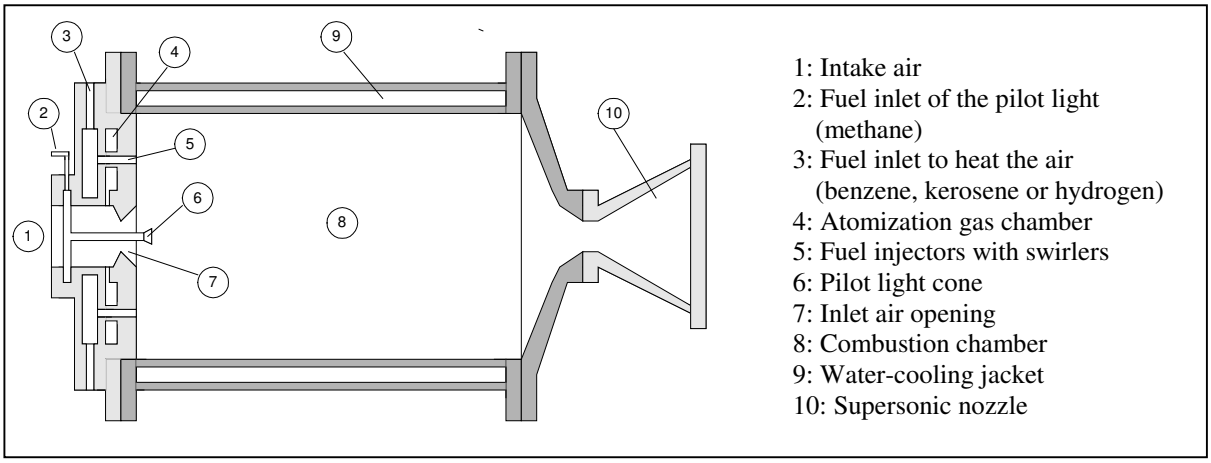

Figure 3: Schematics of the vitiated air generator.

In order to control the combustion products and to better evaluate the desired temperature and the proper fuel to oxidizer (air plus O_2) ratio, in the vitiated air generator, a study was done using the packages PSR and PLUG of the software CHEMKIN III, for benzene (C_6H_6) and hydrogen (H_2), for comparison purposes (Leite, 2003). With this study it is possible to estimate the desired flow properties (temperature and composition) at the exit of the nozzle, calculating the most suitable stagnation conditions and composition of the vitiated air inside the combustion chamber of the VAG, only changing the equivalence ratio and the adjusting the proportion of the air and O_2 in the oxidant.

As it was said before, these conditions of the flow at the exit of the supersonic nozzle of the VAG must simulate the same conditions of the air behind oblique or conical shock waves. Therefore, the purpose of the present work is to obtain the conditions of the air behind a conical shock wave, considering a cone flying with high Mach numbers from 6 to 10, to have the necessary conditions of the vitiated air that will be generated inside the VAG for the tests in the LCP scramjet combustor test bench facility.

In this paper will be presented the analyses of the flow field over a cone at zero angle of attack, flying with hypersonic velocity, using three gas models: a calorically perfect, a thermally perfect and an equilibrium high-temperature one. The resulting system of ordinary differential equations is solved numerically by a Runge-Kutta method. Comparisons between the results provided by the three models will be discussed in order to evaluate the influences of high Mach numbers on the main flow variables.

2. Hypersonic flow over a cone

Supersonic or hypersonic flow around an infinite sharp cone, aligned with the free stream flow direction, generate, when the cone angle and the upstream Mach number fall within certain limits, a conical shock wave attached to the vertex of the cone. Such model is called a Taylor and Maccoll flow (Zucrow, 1977 and Anderson, 1990), as shown in Fig. (4). This is conical flow, which is defined as where all the flow properties are constant along the rays from a given vertex.

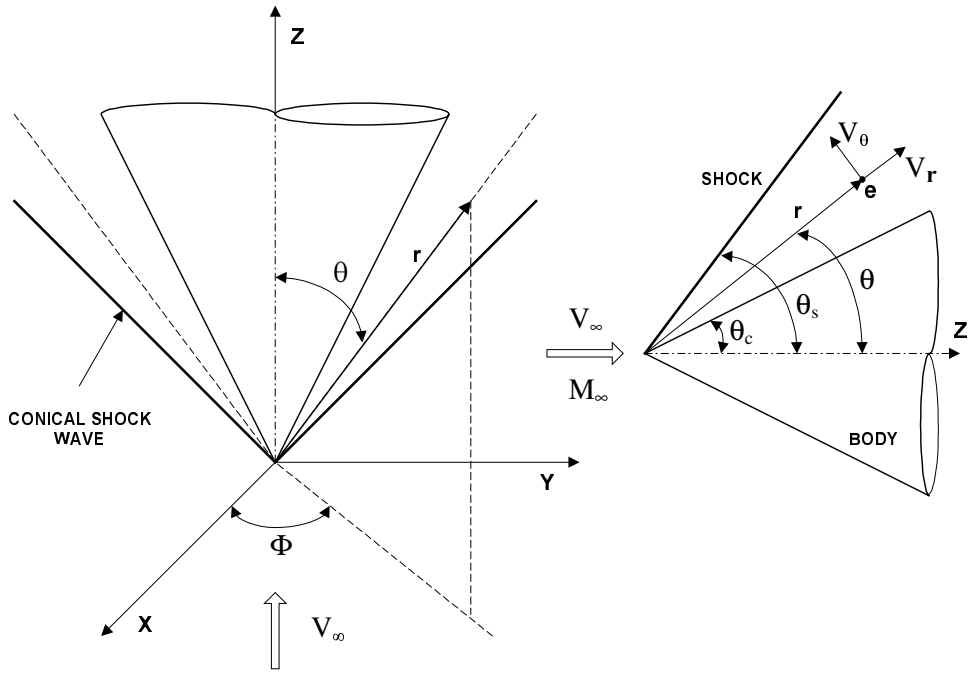

Figure 4: Supersonic flow over a symmetrical cone at zero angle of attack.

The theoretical analysis of a supersonic or hypersonic flow over a cone at zero angle of attack involves solving the equations for steady two-dimensional axisymmetric flow. Numerical solutions of the differential equations have been obtained for a limited numbers of cases and theoretical results are shown to be in good agreement with the experiment (Taylor, 1933 and Sims, 1964).

Figure (4) shows that, as the flow is axisymmetric, the properties are independent of the azimuthal angle Φ and that the ray from the vertex r and the spherical angle θ are the two independent variables. At any point e in the flowfield, the radial and normal components of the velocity are V_r e V_θ, respectively. The semivertex angle of the cone and the shock wave angle, related to z-axis of symmetry, are defined by θ_c and θ_s, respectively.

To solve the conical flowfield between the body and the shock wave it is convenient to express the governing equations in the spherical coordinate system r, θ and Φ.

2.1. The Taylor-Maccoll equation

The continuity equation for the steady flow is given by:

$$\nabla \cdot (\rho \vec{V}) = 0 . \tag{1}$$

In terms of spherical coordinates, Eq. (1) becomes:

$$\nabla \cdot (\rho \vec{V}) = \frac{1}{r^2}\frac{\partial}{\partial r}\left(r^2 \rho V_r\right) + \frac{1}{r \sin\theta}\frac{\partial}{\partial \theta}\left(\rho V_\theta \sin\theta\right) + \frac{1}{r \sin\theta}\frac{\partial (\rho V_\Phi)}{\partial \Phi} = 0 . \tag{2}$$

Evaluating the derivatives, and applying the conditions, given in Eqs. (3) and (4), for axisymmetric conical flow,

$$\frac{\partial}{\partial \Phi} \equiv 0 \tag{3}$$

$$\frac{\partial}{\partial r} \equiv 0 \tag{4}$$

the Eq. (2) becomes:

$$2\rho V_r + \rho V_\theta \cot\theta + \rho \frac{\partial V_\theta}{\partial \theta} + V_\theta \frac{\partial \rho}{\partial \theta} = 0 . \tag{5}$$

Equation (5) is the continuity equation for axisymmetric conical flow.

For steady, inviscid flow with no body forces, Crocco's theorem (Anderson, 1990), is represented by the equation

$$T\nabla s = \nabla h_0 - \vec{V} \times (\nabla \times \vec{V}) . \tag{6}$$

Throughout the conical flowfield $\nabla s = 0$. Moreover, the flow is adiabatic and steady, and hence it can be obtained by the energy equation that $\Delta h_o = 0$. Therefore, Crocco's equation (Eq. (6)) gives that $\nabla \times \vec{V} = 0$, i.e., the conical flow field is irrotational. Since Crocco's theorem is a combination of the momentum and energy equations, then $\nabla \times \vec{V} = 0$ can be used in place of either one. In spherical coordinates,

$$\nabla \times \vec{V} = \frac{1}{r^2 \sin\theta}\begin{vmatrix} e_r & r e_\theta & (r\sin\theta) e_\Phi \\ \frac{\partial}{\partial r} & \frac{\partial}{\partial \theta} & \frac{\partial}{\partial \Phi} \\ V_r & r V_\theta & (r\sin\theta) V_\Phi \end{vmatrix} = 0 \tag{7}$$

where e_r, e_θ and e_Φ are unit vectors in the r, θ and Φ directions respectively.

Expanding Eq. (7), it becomes

$$\nabla \times \vec{V} = \frac{1}{r^2 \sin\theta}\left\{ \begin{array}{l} e_r\left[\frac{\partial}{\partial \theta}(r V_\Phi \sin\theta) - \frac{\partial}{\partial \Phi}(r V_\theta)\right] - r e_\theta\left[\frac{\partial}{\partial r}(r V_\Phi \sin\theta) - \frac{\partial}{\partial \Phi}(V_r)\right] + \\ + (r\sin\theta) e_\Phi\left[\frac{\partial}{\partial r}(r V \theta) - \frac{\partial V_r}{\partial \theta}\right] \end{array} \right\} = 0 . \tag{8}$$

Applying the axisymmetric conical flow conditions (Eqs. (3) and (4)), Eq. (8) simplifies to

$$V_\theta = \frac{\partial V_r}{\partial \theta} \qquad \rightarrow \qquad V_\theta = \frac{dV_r}{d\theta} . \tag{9}$$

Equation (9) is the irrotationality condition for axisymmetric conical flow.

A special form of Euler's equation, which holds for any direction throughout an irrotational inviscid flow with no body forces, is given by Eq. (10) (Anderson, 1990), where p and ρ denotes the pressure and density respectively:

$$dp = -\rho V dV \qquad \rightarrow \qquad (V^2 = V_r^2 + V_\theta^2) . \tag{10}$$

Evaluating the derivative, Eq. (10) becomes

$$dp = -\rho(V_r dV_r + V_\theta dV_\theta) . \tag{11}$$

For isentropic flow, the speed of the sound (a) is given by Eq. (12), where the subscript s denotes constant entropy

$$\frac{dp}{d\rho} \equiv \left(\frac{\partial p}{\partial \rho}\right)_s = a^2 . \tag{12}$$

So, Eq. (11) can be written as

$$\frac{d\rho}{\rho} = -\frac{1}{a^2}(V_r dV_r + V_\theta dV_\theta) . \tag{13}$$

Defining a reference velocity (V_{max}) as the maximum theoretical velocity obtainable from a fixed reservoir condition (when $V = V_{max}$, the flow has expanded theoretically to zero temperature, hence $h = 0$), and as the total enthalpy (h_o) is constant along a given streamline we can have the following equation

$$h_0 = const = h + \frac{V^2}{2} = \frac{V_{max}^2}{2} \qquad \Rightarrow \qquad V_{max} = \sqrt{2h_0} . \tag{14}$$

For a calorically perfect gas that is defined as a gas for which the values of specific heat at constant pressure (c_p) and specific heat at constant volume (c_v) are constants, so the ratio of the specific heats γ is constant, Eq. (14) becomes

$$\frac{a^2}{\gamma - 1} + \frac{V^2}{2} = \frac{V_{max}^2}{2} \qquad \Rightarrow \qquad a^2 = \frac{\gamma - 1}{2}(V_{max}^2 - V^2) = \frac{\gamma - 1}{2}(V_{max}^2 - V_r^2 - V_\theta^2) . \tag{15}$$

Substituting Eq. (15) into Eq. (13)

$$\frac{d\rho}{\rho} = -\frac{2}{\gamma - 1}\left(\frac{V_r dV_r + V_\theta dV_\theta}{V_{max}^2 - V_r^2 - V_\theta^2}\right) . \tag{16}$$

Equations (5), (9) and (16) are three equations with three dependent variables (ρ, V_r and V_θ). Due to the axisymmetric conical flow conditions, there is only one independent variable (θ). Hence, the partial derivatives in the three equations are more properly written as ordinary derivatives.

Combining the three equations (Eqs. (5), (9) and (16)) and considering that if

$$V_\theta = \frac{dV_r}{d\theta} \qquad \Rightarrow \qquad \frac{dV_\theta}{d\theta} = \frac{d^2 V_r}{d\theta^2} . \tag{17}$$

we have

$$\frac{\gamma - 1}{2}\left[V_{max}^2 - V_r^2 - \left(\frac{dV_r}{d\theta}\right)^2\right]\left[2V_r + \frac{dV_r}{d\theta}\cot\theta + \frac{d^2 V_r}{d\theta^2}\right] - \frac{dV_r}{d\theta}\left[V_r \frac{dV_r}{d\theta} + \frac{dV_r}{d\theta}\left(\frac{d^2 V_r}{d\theta^2}\right)\right] = 0 . \tag{18}$$

Equation (18) is the Taylor-Maccoll equation for the solution of conical flows. It is an ordinary differential equation, with only one dependent variable (V_r). Its solution gives $V_r = f(\theta)$ and V_θ can be found by Eq. (9).

To expedite the numerical solution, it is better to define a nondimensional velocity (V') as

$$V' \equiv \frac{V}{V_{max}} . \tag{19}$$

so Eq. (18) can be written in the form given by Eq. (20), where the value of γ, for the air is constant and equal to 1.405

$$\frac{\gamma-1}{2}\left[1-\left(V_r'\right)^2-\left(\frac{dV_r'}{d\theta}\right)^2\right]\left[2V_r'+\frac{dV_r'}{d\theta}\cot\theta+\frac{d^2V_r'}{d\theta^2}\right]-\frac{dV_r'}{d\theta}\left[V_r'\frac{dV_r'}{d\theta}+\frac{dV_r'}{d\theta}\left(\frac{d^2V_r'}{d\theta^2}\right)\right]=0 \tag{20}$$

2.2. Conical flow formulation for a thermally perfect gas

For any diatomic or polyatomic gas the value of c_p (specific heat at constant pressure) and c_v (specific heat at constant volume) actually varies with temperature and can only be approximated as a constant for a relatively narrow temperature range. At some point as the temperature increases, the c_p and c_v values begin to increase due to the excitation of vibrational energy of the molecules. For the air, this phenomena occurs around 800 K. Thus above 800 K, the use of $\gamma = 1.405$ in the calorically perfect gas equations will yield incorrect results. The variation of c_p and c_v with temperature (and only with temperature) continues up to approximately 2000 K, for air at 1 atm pressure (Anderson, 2000). Above this value of temperature the dissociation of the molecules of the air starts to occur. In this temperature range, where the value of c_p and c_v is a function only the temperature, air is considered a thermally perfect gas.

A set of thermally perfect gas equations is derived for the specific heat as a polynomial function of temperature to be used to calculate the properties of the flow behind the conical shock wave. These results will be compared with the ones obtained with the Taylor-Maccoll equation for conical flow for calorically perfect temperature regime.

2.2.1 Polynomial curve fit for c_p

The selection of a suitable curve fit function for c_p is the starting point for the development of thermally perfect compressible flow relations. The form chosen for this work was the eight-term, fifth-order, polynomial expression given by Eq. (21) in which the value of c_p has been nondimensionalized by the species gas constant (Witte, 1994).

$$\frac{c_p}{R}=A_1\left(\frac{1}{T^2}\right)+A_2\left(\frac{1}{T}\right)+A_3+A_4(T)+A_5\left(T^2\right)+A_6\left(T^3\right)+A_7\left(T^4\right)+A_8\left(T^5\right)=\sum_{j=1}^{8}A_jT^{j-3}\ . \tag{21}$$

For a given temperature range, A_1 to A_8 are the coefficients of the curve fit. This is a functional form for c_p (Rate, 1990), which provides values of A_1 to A_8 for 15 different gas species. McBride (1963) provides similar c_p/R coefficient data for over 200 different gas species for a five-term, fourth-order polynomial curve fit equation (A_3 to A_7). Equation (21) is also valid with these coefficients provided that A_1, A_2 and A_8 are set equal to zero. In Eq. (21) R denotes the specific gas constant.

The c_p of a mixture of gases is given by

$$c_{p,mix}=\sum_{i=1}^{n}Y_ic_{p,i} \tag{22}$$

where Y_i is the mass fraction of the i^{th} gas species. The value of $c_{p,i}$ is determined from Eq. (21) for each component species. The following example of the standard air, consisting of the four major component gas species: N_2, O_2, A_r and CO_2.

$$c_{p,air}=Y_{N_2}c_{p,N_2}+Y_{O_2}c_{p,O_2}+Y_{Ar}c_{p,Ar}+Y_{CO_2}c_{p,CO_2}\ . \tag{23}$$

Equation (23) can be fully expanded with the use of Eq. (21) in the form

$$\begin{aligned}c_{p,air}=&Y_{N_2}R_{N_2}A_{1,N_2}\left(\frac{1}{T^2}\right)+Y_{N_2}R_{N_2}A_{2,N_2}\left(\frac{1}{T}\right)+\ldots+Y_{N_2}R_{N_2}A_{8,N_2}T^5+\\&+Y_{O_2}R_{O_2}A_{1,O_2}\left(\frac{1}{T^2}\right)+Y_{O_2}R_{O_2}A_{2,O_2}\left(\frac{1}{T}\right)+\ldots+Y_{O_2}R_{O_2}A_{8,O_2}T^5+\\&+Y_{Ar}R_{Ar}A_{1,Ar}\left(\frac{1}{T^2}\right)+Y_{Ar}R_{Ar}A_{2,Ar}\left(\frac{1}{T}\right)+\ldots+Y_{Ar}R_{Ar}A_{8,Ar}T^5+\\&+Y_{CO_2}R_{CO_2}A_{1,CO_2}\left(\frac{1}{T^2}\right)+Y_{CO_2}R_{CO_2}A_{2,CO_2}\left(\frac{1}{T}\right)+\ldots+Y_{CO_2}R_{CO_2}A_{8,CO_2}T^5\end{aligned}\ . \tag{24}$$

Combining like terms in Eq. (24), a resultant c_p curve fit for gas mixture, i.e. for air, is generated. For convenience, the specific heat at constant pressure for thermally perfect gas will be represented by $\tilde{c}_p$.

$$\tilde{c}_{p,air} = A_{1,air}\left(\frac{1}{T^2}\right) + A_{2,air}\left(\frac{1}{T}\right) + A_{3,air} + A_{4,air}(T) + A_{5,air}\left(T^2\right) + A_{6,air}\left(T^3\right) + A_{7,air}\left(T^4\right) + A_{8,air}\left(T^5\right). \tag{25}$$

where

$$A_{j,air} = Y_{N_2} R_{N_2} A_{j,N_2} + Y_{O_2} R_{O_2} A_{j,O_2} + Y_{Ar} R_{Ar} A_{j,Ar} + Y_{CO_2} R_{CO_2} A_{j,CO_2}\,. \tag{26}$$

2.2.2. Isentropic relations

If the flow is assumed to be adiabatic, then the energy equation for two separate points in the flowfield is

$$h_1 + \frac{V_1^2}{2} = h_2 + \frac{V_2^2}{2}. \tag{27}$$

Using the definition of h reference to 0 K, where $h = \int c_p dT$ represents the enthalpy, it gives

$$\int_0^{T_1} \tilde{c}_p dT + \frac{V_1^2}{2} = \int_0^{T_2} \tilde{c}_p dT + \frac{V_2^2}{2}\,. \tag{28}$$

If point 2 is selected to represent the stagnation condition, then $V_2 = 0$ and $T_2 = T_t$. Then Eq. (28) reduces to

$$\frac{V_1^2}{2} = \int_0^{T_t} \tilde{c}_p dT - \int_0^{T_1} \tilde{c}_p dT = \int_{T_1}^{T_t} \tilde{c}_p dT \qquad \Rightarrow \qquad V_1 = 2\sqrt{\int_{T1}^{Tt} \tilde{c}_p dT} \tag{29}$$

where for the selected fifth-order curve fit for $\tilde{c}_p$ (Eq. (25)), the factor $\int_{T_1}^{T_t} \tilde{c}_p dT$ becomes

$$\begin{aligned}\int_{T_1}^{T_t} \tilde{c}_p dT = &-A_1\left(\frac{1}{T_t} - \frac{1}{T_1}\right) + A_2 \ln\frac{T_t}{T_1} + A_3(T_t - T_1) + \frac{A_4}{2}\left(T_t^2 - T_1^2\right) + \frac{A_5}{2}\left(T_t^3 - T_1^3\right) + \frac{A_6}{2}\left(T_t^4 - T_1^4\right) + \\ &+ \frac{A_7}{2}\left(T_t^5 - T_1^5\right) + \frac{A_8}{2}\left(T_t^6 - T_1^6\right)\end{aligned} \tag{30}$$

With knowledge of $\tilde{\gamma}$ (ratio of the specifics hearts for the thermally perfect gas) that can be calculated using the value of $\tilde{c}_p$ obtained from Eq. (25) in the relation

$$\tilde{\gamma} = \frac{\tilde{c}_p}{\tilde{c}_p - R} \tag{31}$$

and with the knowledge of the speed of the sound for thermally perfect gas ($\tilde{a}_1$) given by the relation

$$\tilde{a}_1 = \sqrt{\tilde{\gamma} R T_1} \tag{32}$$

the Mach number can be obtained along with V_1 from Eq. (29).

An expression for the static to total pressure ratio (p_1/p_t) is obtained through the use of the first law of thermodynamics, the definitions of enthalpy and entropy, the equation of state, and the assumption of isentropic flow (Witte, 1994).

$$\frac{p_1}{p_t} = \frac{1}{exp\left(\frac{1}{R}\int_{T1}^{Tt} \frac{\tilde{c}_p}{T} dT\right)} \tag{33}$$

For the selected fifth-order curve fit for $\widetilde{c}_p$, the integral in Eq. (33) becomes

$$\int_{T_1}^{T_t}\frac{\widetilde{c}_p}{T}dT = -\frac{A_1}{2}\left(\frac{1}{T_t^{\,2}}-\frac{1}{T_1^{\,2}}\right)-A_2\left(\frac{1}{T_t}-\frac{1}{T_1}\right)+A_3\,ln\frac{T_t}{T_1}+A_4(T_t-T_1)+\frac{A_5}{2}\left(T_t^{\,2}-T_1^{\,2}\right)+\frac{A_6}{3}\left(T_t^{\,3}-T_1^{\,3}\right)+$$
$$+\frac{A7}{4}\left(T_t^{\,4}-T_1^{\,4}\right)+\frac{A_8}{5}\left(T_t^{\,5}-T_1^{\,5}\right) \tag{34}$$

2.2.3. Conical flow for thermally perfect gas

As it was said before, for a thermally perfect gas, the specific heat at constant pressure ($\widetilde{c}_p$) is a function only the temperature and is given by Eq. (25). The ratio of the specific heats ($\widetilde{\gamma}$) and the speed of the sound ($\widetilde{a}$) for thermally perfect gas are defined by Eqs. (31) and (32) respectively. Following the same development of the Taylor-Maccoll equations, for calorically perfect gas, it is possible to write the thermally perfect gas conical flow equation, considering the relations defined in section 2.2.2., as

$$\frac{\widetilde{\gamma}-1}{2}\left[V_{max}^2-V_r^2-\left(\frac{dV_r}{d\theta}\right)^2\right]\left[2V_r+\frac{dV_r}{d\theta}cot\,\theta+\frac{d^2V_r}{d\theta^2}\right]-\frac{dV_r}{d\theta}\left[V_r\frac{dV_r}{d\theta}+\frac{dV_r}{d\theta}\left(\frac{d^2V_r}{d\theta^2}\right)\right]=0\,. \tag{35}$$

where the value of $\widetilde{\gamma}$ is given by Eq. (31) and then the value of V_θ can be found by Eq. (9).

2.3. Conical flow formulation for a gas in equilibrium

For the air at 1 atm, when the temperature reaches about 2000 K, the dissociation of O_2 begins (Anderson, 2000). At 4000 K, the O_2 dissociation is essentially complete, most of the oxygen is in the form of atomic oxygen O and the dissociation of N_2 begins. If the pressure is increased the dissociations of the O_2 and N_2 begin at higher temperatures and for lower pressures it the dissociation occurs also at lower temperatures. For this case, considering the gas in equilibrium, the chemical composition is a unique function of both the temperature and the pressure. For a thermodynamic system in equilibrium (including an equilibrium chemically reacting system), the state of the system is uniquely defined by any two states variables.

2.3.1 Equilibrium thermodynamic properties of high-temperature air

A particularly convenient method of entering high-temperature equilibrium air properties into the flowfield calculation is by way of polynomial correlations of the calculated and tabulated data (Tannehill, 1972 and 1974).

In terms of specific enthalpy as a function of pressure and density, i.e., $h = h(p,\rho)$ we have

$$h=\frac{p}{\rho}\left[\frac{\widetilde{\widetilde{\gamma}}}{\widetilde{\widetilde{\gamma}}-1}\right] \tag{36}$$

where

$$\widetilde{\widetilde{\gamma}}=c_1+c_2Y+c_3Z+c_4YZ+\frac{c_5+c_6+c_7Z+c_8YZ}{1+exp\left[c_9\left(X+c_{10}Y+c_{11}\right)\right]} \tag{37}$$

and where $Y=log_{10}\left(\rho/1.292\right)$, $X=log_{10}\left(p/1.013x10^5\right)$ and $Z=X-Y$.

The unit for p is N/m^2, the unit for ρ is kg/m^3 and the coefficients c_1, c_2, …, c_{11} are tabulated in reference (Anderson, 2000).

The ratio of the specifics hearts for the gas in equilibrium is represented here by $\widetilde{\widetilde{\gamma}}$ to be distinguished from $\widetilde{\gamma}$ for the thermally perfect gas and from γ for the calorically perfect gas.

In terms of temperature as a function of pressure and density, we have

$$log_{10}\left(\frac{T}{151.78}\right)=d_1+d_2Y+d_3Z+d_4YZ+d_5Z^2+\frac{d_6+d_7Y+d_8Z+d_9YZ+d_{10}Z^2}{1+exp\left[d_{11}\left(Z+d_{12}\right)\right]}\,. \tag{38}$$

where $Y = \log_{10}\left(\rho / 1.292\right)$, $X = \log_{10}\left(p / 1.013x10^5\right)$ and $Z = X - Y$. The coefficients d_1, d_2, …, d_{12} are tabulated in reference (Anderson, 2000).

A correlation for the equilibrium speed of sound in high-temperature air is given by (Tannehill, 1974)

$$a = \left[e\left\{ K_1 + \left(\tilde{\tilde{\gamma}} - 1\right)\right)\left[\tilde{\tilde{\gamma}} + K_2\left(\frac{\partial \tilde{\tilde{\gamma}}}{\partial \ln e} \right)_\rho \right] + K_3\left(\frac{\partial \tilde{\tilde{\gamma}}}{\partial \ln \rho} \right)_e \right\} \right]^{1/2} . \tag{39}$$

The coefficients K_1, K_2 e K_3 are tabulated also in reference (Anderson, 2000) and $\tilde{\tilde{\gamma}}$ is defined by Eq. (37).

2.2.3. Equilibrium conical flow

Consider the equilibrium high-temperature supersonic or hypersonic flow over a cone at zero degrees angle of attack. The classical model of conical flow, Taylor-Maccoll, can be considered.

The governing equations, for axisymmetric conical flow, of continuity and r direction momentum are the same obtained in section 2.1. So, for conical flow in spherical coordinates, the continuity equation is given by Eq. (5) and the r-direction momentum equation is given by Eq. (9).

The θ-direction momentum equation, in spherical coordinates, is given by

$$V_r \frac{\partial V_\theta}{\partial r} + \frac{V_\theta}{r}\frac{\partial V_\theta}{\partial \theta} + \frac{V_r V_\theta}{r} = -\frac{1}{\rho r}\frac{\partial p}{\partial \theta} \tag{40}$$

and applying the conical flow assumption, Eq. (40) becomes

$$V_\theta \frac{dV_\theta}{d\theta} + V_r V_\theta = -\frac{1}{\rho}\frac{dp}{d\theta} \tag{41}$$

Equation (41) is the θ-direction momentum equation for conical flow.

Considering isentropic the flow between the shock and the cone, any change in pressure, dp, in any direction in the flowfield is related to a corresponding change in density, $d\rho$, via the speed of sound relation given by Eq. (12).

With Eq. (12), Eq. (5) can be written as

$$2V_r + V_\theta \cot\theta + \frac{dV_\theta}{d\theta} + \frac{V_\theta}{\rho a^2}\frac{dp}{d\theta} = 0 \tag{42}$$

Equations (41) and (42) are two equations in terms of the derivatives $dV_\theta / d\theta$ and $dp / d\theta$. Solving Eqs. (41) and (42) for these derivatives, it gives

$$\frac{dV_\theta}{d\theta} = \frac{a^2}{V_\theta^2 - a^2}\left(2V_r + V_\theta \cot\theta - \frac{V_r V_\theta^2}{a^2} \right) \tag{43}$$

and

$$\frac{dp}{d\theta} = -\frac{\rho V_\theta a^2}{V_\theta - a^2}\left(V_r + V_\theta \cot\theta\right) \tag{44}$$

Equations (9), (43) and (44) constitute three coupled ordinary differential equation in terms of the five unknowns, V_θ, V_r, p, ρ and a. This system is completed by adding the equilibrium high-temperature thermodynamic properties in the form of $\rho = \rho(p,h)$, given by Eqs. (36) and (37) and $a = a(e,\rho)$ given by Eq. (39) and that system of five equations represent the governing equations for equilibrium flow over a cone.

3. Numerical solution of the conical flow equations

The present study was performed to find the conditions behind the conical shock wave formed over the vertex of a circular cone with 15-degree semi angle flying at Mach numbers from 6 to 10. These conditions, specially the values of temperature and Mach number, are the ones that should be generated at the exit of the nozzle of the vitiated air generator (VAG). These generated conditions, at the exit of the nozzle, should be the most similar as possible to the conditions, in the real flight, at the entrance of the scramjet combustors, where the supersonic combustion will take place. The conditions to be simulated should also account for the flight altitude since, at low pressures, the O_2 and N_2 dissociations begin to occur earlier, i.e., the lower is the pressure, the lower is the temperature that the dissociation of the air begin to occur, and when it happens the properties of the flow have to be calculated, considering the equilibrium flow model.

To illustrate the variation of the specific heat ratios (γ) with temperature and pressure, Fig. (5) shows $\gamma = \boldsymbol{c}_p / \boldsymbol{c}_v$, immediately behind an oblique shock wave, as a function of the shock wave angle and the Mach number, for two different altitudes conditions, one at the sea level (H = 0 m) and another for H = 10000 m (NASA/NOAA/USAF, 1976).

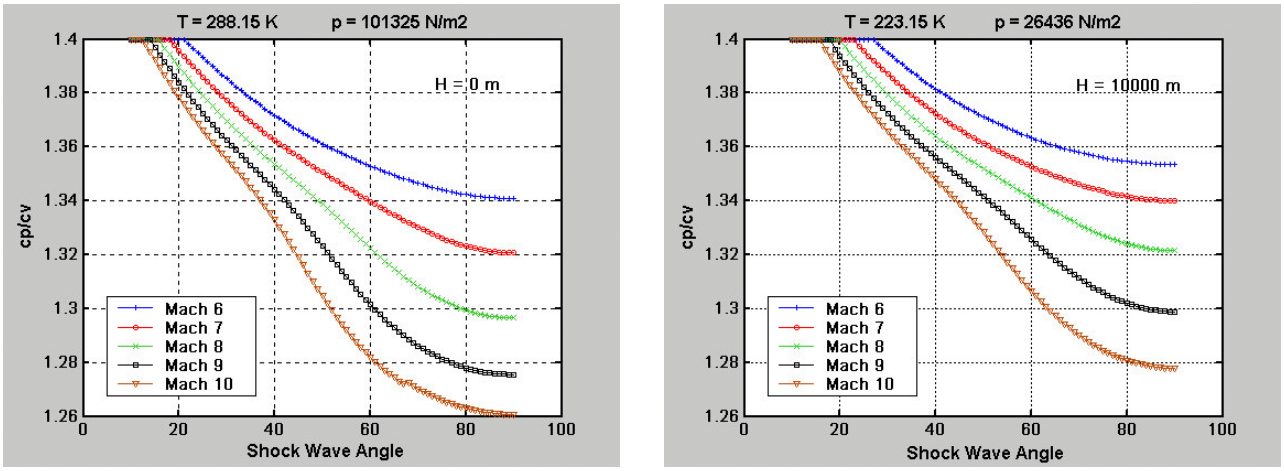

Figure 5: Ratio of specific heats for two different altitudes.

For the numerical solution of the supersonic or hypersonic flow over a circular cone, for the three models (calorically perfect, thermally perfect and in equilibrium), it was employed the inverse approach, where assuming a shock angle, the particular cone that supports the given shock is calculated. This is a contrast to the direct approach, where the cone angle is given and the flowfield and the shock wave angle are calculated.

For each one of the three flow models it was assumed a value for the shock wave angle (θ_s) and the conditions of the flow immediately behind the shock were found from the oblique shock relations: for calorically perfect (Anderson, 1990), for thermally perfect (Tatum, 1997) and for equilibrium gas (Anderson, 2000). Using the values found for the component of the velocity in $\boldsymbol{r}$ direction ($\boldsymbol{V}_r$) and in θ direction ($\boldsymbol{V}_\theta$) and for the sound speed ($\boldsymbol{a}_2$) and pressure ($\boldsymbol{p}_2$), immediately behind the shock wave, as initial values, Eq. (20), for the calorically perfect flow, Eq. (35), for thermally perfect flow and Eqs. (43) and (44), for the flow in equilibrium were solved numerically in steps of θ, marching away from the shock to the cone surface. The flow field between the shock and cone was divided into incremental angles $\Delta\theta$ and the equations were solved by a Runge-Kutta method.

At each increment in θ, the value of $\boldsymbol{V}_\theta$ is calculated, for a given free stream Mach number $\boldsymbol{M}_\infty$. At some value of θ we have that the value of the normal component of the velocity related to the shock wave is $\boldsymbol{V}_\theta = \boldsymbol{0}$. When it happens $\theta = \theta_c$, where θ_c represents the angle of the surface of the particular cone, which supports the shock wave of a given shock wave angle (θ_s) at a given Mach number ($\boldsymbol{M}_\infty$). So, θ_c is the cone angle compatible with the $\boldsymbol{M}_\infty$ and θ_s given. The value of the component of the velocity in $\boldsymbol{r}$ direction ($\boldsymbol{V}_r$) at θ_c gives the Mach number along the cone surface. With this process, the complete flowfield between the shock and the body can be obtained.

The process described above was used for the three flow models: calorically perfect, thermally perfect and in equilibrium. Some of the results obtained for the semi angle of the cone, θ_c = 15, were plotted below as a function of the free stream Mach numbers. For these calculations it were used the free stream conditions relative to the sea level altitude where the temperature is 288.15 K, the pressure is 101325 N/m^2 and the density is 1.225 kg/m^3.

Figure (6) shows the comparison between the conditions behind the conical shock wave for the three flow models: the calorically perfect, where γ is considered to be constant and equal to 1.405, the thermally perfect, where $\tilde{\gamma}$ is a function only of the temperature and the equilibrium flow model, where $\tilde{\tilde{\gamma}}$ is a function of the temperature and the pressure.

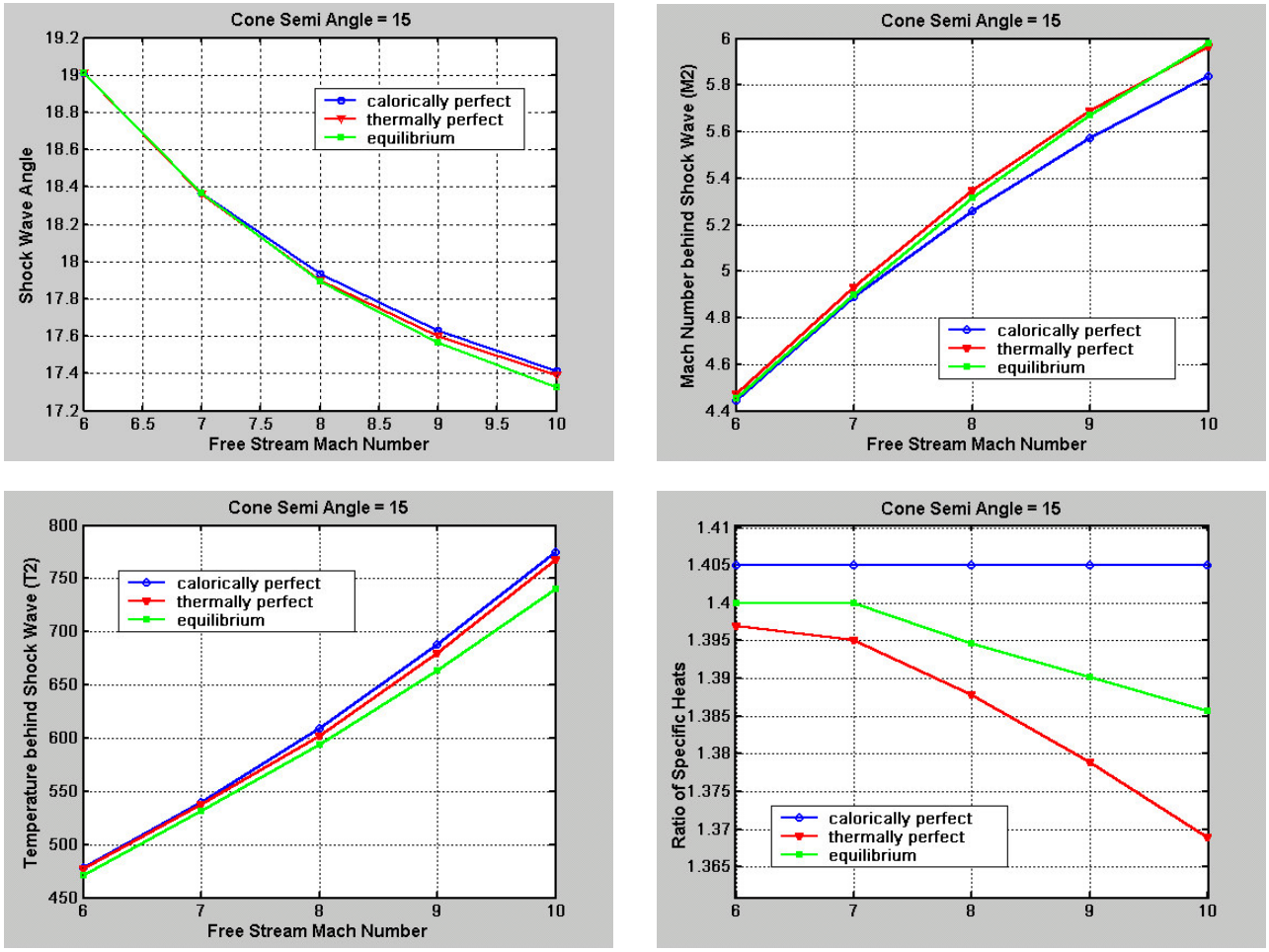

Figure 6: Comparison of the flow conditions behind the conical shock wave for the three models: calorically perfect, thermally perfect and equilibrium for $p_\infty = 1$ atm and $T_\infty = 288.15$ K.

To solve the equations it was developed, for the three models, an algorithm using the mathematic software tool MATLAB. The results obtained for the calorically perfect model were compared with the ones tabulated in Sims (1964) with excellent agreement, as shown in Tab. (1). The values were calculated for a cone with 15-degree semi angle flying at Mach numbers from 6 to 10 and were presented on Tab. (1), on the left column of each Mach number, where the subscript ∞ refers to the free stream conditions, the subscript ***2*** refers to the flow behind the conical shock wave and ***s*** to the shock.

Table 1: Comparison between calculated values (using a calorically perfect model) and tabulated values (Sims, 1964) for a cone with 15-degree semi angle flying at Mach numbers 6, 7, 8 and 10.

	$M_\infty = 6$		$M_\infty = 7$		$M_\infty = 8$		$M_\infty = 10$	
	Calculated Values	Tabulated Values	Calculated Values	Tabulated Values	Calculated Values	Tabulated Values	Calculated Values	Tabulated Values
θ_s	19.0070	19.0072	18.3640	18.3643	17.9330	17.9339	17.4120	17.4126
M_2	4.4446	4.4542	4.8871	4.8997	5.2604	5.2758	5.8378	5.8586
ρ_2/ρ_∞	2.5895	2.5981	2.9465	2.9586	3.2738	3.2895	3.8275	3.8503
p_2/p_∞	4.2932	4.2883	5.5143	5.5078	6.9209	6.9128	10.2940	10.2810
T_2/T_∞	1.6579	1.6506	1.8715	1.8616	2.1140	2.1014	2.6895	2.6702

For the others two models it is difficult to have tables to compare the calculated values because for the thermally perfect model we have a different value for each temperature and for the equilibrium flow model we have, for the same temperature, a different value for each pressure, but the procedure of calculation for the these two last models was the same used for the calorically perfect one, changing only the equations relative to each model, showed in sections 2.2 and 2.3.

4. Conclusions

The main goal of this work was to obtain the values of temperature and Mach number behind the conical shock wave, so with this, we can have the conditions to be generated at the exit of the nozzle of the vitiated air generator (VAG). With the value of the temperature it is possible to predict, for each experiment using the VAG, the equivalence ratio between the oxidant and fuel, to obtain the stagnation temperature, in the combustion chamber of the VAG, before passing through the nozzle (Fig. (3)). Also with the value of the temperature we can calculate the composition of the air for that temperature and with that estimate the composition of the oxidant, i.e., the proportion between the air and oxygen (O_2) used to enrich the air inside the combustion chamber of the VAG, to keep the same composition of the air after the combustion at the exit of the nozzle. With the values of the Mach number behind the conical shock wave, calculated in this work, it is possible to design the nozzles necessary for the experiments.

Figure (6) shows, for cones with 15-degree semi angle, that for experiments where the free stream Mach numbers ($\boldsymbol{M}_\infty$) are below 7, at sea level pressure, it is possible to consider the flow behind the shock as calorically perfect. For values of the free stream Mach numbers higher than 7 it is better to consider the flow behind the shock as a thermally perfect or in equilibrium one, taking into account the temperature and also the pressure of the flow behind the shock wave.

5. References

Anderson, J. D. Jr., 1990, "Modern Compressible Flow", McGraw-Hill Book Co., New York.

Anderson, J. D. Jr., 2000, "Hypersonic and High Temperature Gas Dynamics", American Institute of Aeronautics and Astronautics.

Dunsworth, L. C., Reed, G. J., 1979, "Ramjet Engine Testing and Simulation Techniques", Journal of Spacecrafts and Rockets, 6 (16), pages 382-388.

Guimarães, A. L. S., Bastos-Netto, D., Sinay, L. R., 1993, "Aquecedores de Ar para Experimentos em Combustão Supersônica", Proceedings of the 45th Anual Meeting of the Brasilian Society for Science Development, Recife, Brazil.

Guimarães, A. L. S., 1996, "Modelagem de um Aquecedor para Banco de Testes de Estato-Reatores a Combustão Supersônica", MSc. Dissertation, National Institute for Space Research (INPE), São José dos Campos, Brazil.

Guimarães, A. L. S., Sinay, L. R., Bastos-Netto, D., jul/1997, "Liquid Fuel Burner with Oxygen Replenishment for Testing Scramjets Combustors", 33rd AIAA/ASME/SAE/ASEE Joint Propulsion Conference and Exhibit, Seatttle, WA, USA, Paper AIAA 97-3020.

Guimarães, A. L. S., Sinay, L. R., Bastos-Netto, D., dec/1997, "A Simple One-Dimensional Model for Liquid Fuel Vitiated Air Heater for Scramjets Direct-Connected Test Facilities", 4th Asian-Pacific International Symposium on Combustion and Energy Utilization, Bangkok, Thailand.

Heiser, W. H., Pratt, D. T., 1994, "Hypersonic Airbreathing Propulsion", AIAA Education Series.

Hertzberg, A., Bruckner, A. P. and Bogdanoff, D. W., 1988, "Ram Accelerator: A New Chemical Method for Accelerating Projectiles to Ultrahigh Velocities", AIAA Jounal, Vol. 26, No. 2, pp. 195-203.

Leite, V. S. F. O., Bastos-Netto, D., 2003, "Numerical Evaluation of the Combustion Process in a Vitiated Air Generator of a Direct-Connected Supersonic Combustion Reserach Facility", Proceedings of the 17th Brazilian Congress of Mechanical Engineering, COBEM, São Paulo, Brazil.

McBride, B. J., Heimel, S, Ehlers, J. G., Gordon, S., 1963, "Thermodynamic Properties to 6000 K for 210 Substances Involving the First 18 Elements", NASA SP-3001.

NASA, NOAA, USAF, 1976, "U. S. Standard Atmosphere", Washington D.C., Government Printing Office.

Rate Constant Committee, NASP High-Speed Propulsion Technology Team, 1990, "Hypersonic Combustion Kinetics", NASP TM-1107.

Sims, J. L., 1964, "Tables for Supersonic Flow Around Right Circular Cones at Zero Angle of Attack", NASA SP-3004.

Tannehill, J. C., Mohling, R. A., 1972, "Development of Equilibrium Air Computer Programs Suitable for Numerical Computation Using Time-Dependent or Shock-Capturing Methods", NASA CR-2134.

Tannehill, J. C., Mugge, P. H., 1974, "Improved Curve Fits for Thermodynamic Properties of Equilibrium Air Suitable for Numerical Computation Using Time-Dependent or Shock-Capturing Methods", NASA CR-2470.

Tatum, K. E., 1997, "Computation of Thermally Perfect Oblique Shock Wave Properties", 35th Aerospace Sciences Meeting and Exhibit, Reno, AIAA-97-0868.

Taylor, G. I., Maccoll, J. W., 1933, "The Air Pressure on a Cone Moving at High Speed", Proceedings of the Royal Society of London, series A,, vol. 139, pp. 278-311.

Witte, D. W., Tatum, K. E., 1994, "Computer Code for Determination of Thermally Perfect Gas Properties", Langley Research Center, NASA Technical Paper 3447.

Zucrow, M. J., Hoffman, J. D., 1977, "Gas Dynamics", vol. 2, School of Mechanical Engineering Purdue University, John Wiley & Sons.